ChemComm

Simultaneous self-exfoliation and autonomous motion of MoS2 particles in water

Journal:	*ChemComm*
Manuscript ID:	CC-COM-04-2015-003401.R1
Article Type:	Communication
Date Submitted by the Author:	06-May-2015
Complete List of Authors:	Wang, Hong; Nanyang Technological University, Division of Chemistry and Biological Chemistry Moo, James Guo Sheng; Nanyang Technological University, Division of Chemistry and Biological Chemistry Sofer, Zdenek; Institute of Chemical Technology, Prague, Department of Inorganic Chemistry Pumera, Martin; Nanyang Technological University, Chemistry and Biological Chemistry

Journal Name

RSCPublishing

COMMUNICATION

Simultaneous self-exfoliation and autonomous motion of MoS_2 particles in water

Cite this: DOI: 10.1039/xoxxoooooox

Hong Wang,[a] Zdenek Sofer,[b] James Guo Sheng Moo, [a] and Martin Pumera[a]

Received ooth January 2012,
Accepted ooth January 2012

DOI: 10.1039/xoxxoooooox

www.rsc.org/

Two-dimensional (2D) transitional metal dichalcogenides (TMDCs) have been receiving significant research interest due to their unique physical and electronic properties. We report the design of a MoS_2 based motor that can display simultaneous self-exfoliation and autonomous motion at the surface of water. Exfoliation of bulk MoS_2 via sodium intercalation offers an attractive way to obtain solution-phase 2D MoS_2 nanosheets in large scale. The motion of the MoS_2 particle results from the surface tension gradients generated by the naphthalene distributed in the MoS_2 particles. Combination of the self-exfoliation and propulsion in unmodified water environment hence leads to a new platform which holds great promise for new applications of TMDC materials and small scale motors.

Transition metal dichalcogenides are layered materials with strong bonding in each layer and weak interactions between the layers, enabling exfoliation into two-dimensional nanosheets with the chalcogen atoms in two hexagonal planes separated by a plane of metal atoms.[1] Because of the unusual electronic, optical, mechanical, chemical and thermal properties,[2, 3] TMDCs have been an emerging class of materials with a range of potential applications in recent years.[4] For molybdenum disulfide (MoS_2), a widely known layered transition metal dichalcogenide, each Mo atom is coordinated by six S-atoms in either a trigonal prismatic or octahedral system by covalent bonds within each layer, while van der Waals interaction connects the adjacent layers.[5] The electronic properties of 2D layered nanomaterials are highly associated with their thickness.[6] Single layer MoS_2 and bulk MoS_2 are inherently different materials with large changes in properties. The band gap of MoS_2 increases with decreasing the thickness of the material and there exists a transition from an indirect band gap in the bulk form to a direct band gap in the monolayer.[7] The direct band gap, high current on/off ratios, large in-plane carrier mobility and robust mechanical properties of single layer MoS_2[8-11] open up new prospects for practical applications in novel field effect transistors[12, 13] and optoelectronic devices.[14-16]

Exfoliation of bulk MoS_2 into 2D layered nanosheets represents a critical step towards translating their unique properties into applications. Individual MoS_2 monolayers of high purity can be peeled from bulk crystals by micromechanical cleavage using adhesive tapes, but this method suffers from the problem of scalability and lack of control.[17-19] Solution-phase preparations provide a promising alternative to obtain exfoliated nanosheets in large scale.[20-22] The intercalation of MoS_2 by alkali metal allows the layers to be exfoliated in liquid.[23] The intercalation of alkali metal into the host laminar structure of MoS_2 can be achieved by either use of hot alkali metal vapor[24] or through soaking the bulk material in a solution of the corresponding alkali metal-containing compound, typically, in solvated metal ammonia solution or a hexane solution of butyl lithium.[25, 26] An electrochemical intercalation approach has also been developed with the advantages of being able to monitor and control the intercalation process.[22] Once the alkali metal is intercalated into MoS_2, the material is ready for exfoliation. The H_2 gas evolution upon exposing the intercalated material to water rapidly separates the layers, resulting in a dispersed suspension of 2D layers of MoS_2. As an alternative precursor for liquid phase exfoliation, ammoniated MoS_2 can be exfoliated readily in a variety of polar solvents due to the fact that the intercalated NH_3/NH_4^+ can invite solvent molecules into the interlayer and the evolution of ammonia gas during sonication would facilitate the exfoliation.[27]

Recent efforts have demonstrated the great potential of MoS_2 to be involved in biomedical applications. Defect sites arising from the loss of sulphur atoms are available for surface modification by thiolated compounds.[28] MoS_2 nanosheets functionalized with lipoic acid-terminated polyethylene glycol (LA-PEG) have shown high stability in physiological solutions without obvious cytotoxicity.[29] The high surface area suitable for drug loading and strong near-infrared (NIR) absorbance of two-dimensional MoS_2 nanosheets make them a promising candidate for combined photothermal and chemotherapy of cancer.[30] Functionalized MoS_2 based biosensors have been used for detection of DNA and other biomolecules, providing new opportunities in bioanalysis and clinic diagnosis field.[31-33] In addition, MoS_2 is also a promising material for environmental remediation. It has been shown that intercalated MoS_2 can be used as redox-recyclable ion-exchange materials for the extraction of aqueous heavy metal ions.[34]

Micro/nanomotors, which are micro- or nanoscale devices capable of converting energy into mechanical forces and movement, attract considerable interests as an emerging solution to address problems

encountered in many fields, especially in biomedical and environmental area.[35] Designing and fabricating micro/nanomotors represents one of the most significant challenges facing nanotechnology. Among various reported micro/nanoscale motors, particular attention has been given to self-propelled micro/nanomotors relying on chemical reactions to harvest energy. Different types of small-scale self-propelled objects, such as striped nanorods, Janus particles and tubular microjets, have been developed on the basis of self-electrophoresis, self-diffusiophoresis and bubble ejection.[36] However, in the vast majority of the existing cases, metals, especially noble metals, are employed as indispensable components in the structure of the micro/nanomotors. In addition, the commonly used hydrogen peroxide fuel is toxic, which hinders the development of practical applications of these promising tiny motors. New alternative fuels, including Br_2, I_2, hydrazine, as well as acidic and alkaline solutions,[37-39] have been put forward to replace hydrogen peroxide. Here, as an initial proof of concept, we report a millimeter-sized TMDC-based motor that exhibit self-propulsion in water. The intercalated MoS_2 particles exhibit fast autonomous motion during the self-exfoliation process in water. In the following sections, we will characterize the fabrication and movement of the MoS_2 based motors.

Sodium intercalated MoS_2 prepared with the use of sodium naphthalenide was employed in this study. The intercalation of sodium into MoS_2 may be regarded as an ion/electron transfer topotactic reaction. The driving force for the intercalation reaction is suggested to be the tendency for charge transfer from sodium to the host MoS_2 lattice.[5, 24] The electrons from the sodium are transferred to the lowest lying unoccupied energy levels of the MoS_2, which are mainly transition metal d bands. Sodium naphthalenide is a kind of electron transfer agents in which sodium transfers an electron to the aromatic system. The resulting radical anion is an electron donor with strong reducing properties. Through the radical anion, the electron from sodium is expected to transfer to MoS_2, followed by the sodium ion intercalating to balance the charge.[40] Except for the electron transfer from the intercalant sodium to the host MoS_2, another effect of intercalation is the expansion of the interlayer spacing and weakened van der Waals interactions between the layers.[24] To prepare the MoS_2 based motor, MoS_2 was submerged in tetrahydrofuran solutions of sodium naphthalenide to insert sodium into the layered structure. The morphology of the resulting sodium intercalated MoS_2 is examined by scanning electron microscopy (SEM). Figure 1A, B and C illustrate the surface characteristics of the intercalated MoS_2 before exfoliation at different magnifications. The bulk materials are stacks of many micro-sized plates and each plate is in fact composed of many monolayers of MoS_2. The typical height of a single layer MoS_2 is reported to be less than 1 nm.[41]

The sodium intercalated MoS_2 exhibits a remarkable ability to exfoliate in water. The exfoliation process is not a purely mechanical process, but a chemical one relying on redox reactions. The reaction of water with the intercalated sodium between the layers generates hydrogen gas, which will force the separation of MoS_2 layers.[42] Meanwhile, the MoS_2 layers undergo oxidation along with hydration.[5, 24] As the reaction proceeds further into the interlayer spaces, the layers become increasing spatially separated and eventually turned into individual single layer or few layers of MoS_2, resulting in a colloidally dispersed suspension. In our study, we used MoS_2 particles with an average diameter of around 2.5 mm. Once immersed in water, the particles undergo a self-exfoliation process. Figure 1 D shows the optical image of the resulting aqueous MoS_2 suspension containing MoS_2 flakes exfoliated to varying degrees. The different optical contrast of the flakes is attributed to the difference in their thickness, which is governed by the number of layers. Further investigation by scanning transmission electron microscopy (STEM) demonstrates the existence of exfoliated flakes with smaller size (Figure 1E, F). Figure 1E displays some partially exfoliated MoS_2 flakes while Figure 1F shows more transparent flakes indicating higher degrees of exfoliation. The average thickness of the exfoliated flakes was characterized by atomic force microscopy (AFM) to be around 1.4 nm (See supporting information for details).

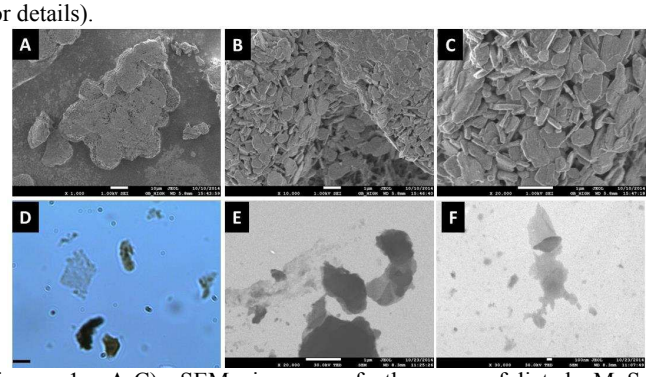

Figure 1. A-C) SEM images of the pre-exfoliated MoS_2 microparticles. Scale bars are 10 μm, 1μm and 1μm, respectively. D) Optical image of Na-exfoliated MoS_2 dispersion in water. Scale bar is 10 μm. E, F) STEM images of Na-exfoliated MoS_2. Scale bars are 1 μm and 100 nm, respectively.

Upon exposure to water, the MoS_2 particles exhibit fast motion while simultaneously experiencing exfoliation. Figure 2 illustrates the trajectories of the movement of the MoS_2 particles in deionized water, which can be either translational (SI video-1) or rotational motion (SI video-2). As the sodium intercalated MoS_2 will exfoliate in water, the size of the particle decreases during motion and the continuous motion is observed until the particle totally disappears. Accordingly, the lifetime of the MoS_2 particle is influenced by the size of the particle. It generally needs more time for larger MoS_2 particles to be exfoliated in water, thus allowing longer lifetimes. For the MoS_2 particles with average diameters of around 2.5 mm used here, the motion and exfoliation process can last for 20-30 seconds. Although the intercalated sodium reacts with water to generate molecular hydrogen and sodium hydroxide, bubbles were not observed during the motion of the MoS_2 particles. We also examined the motion of smaller particles under microscope and bubbles were still not seen, which demonstrates that bubble propulsion is not the main driving force for the motion.

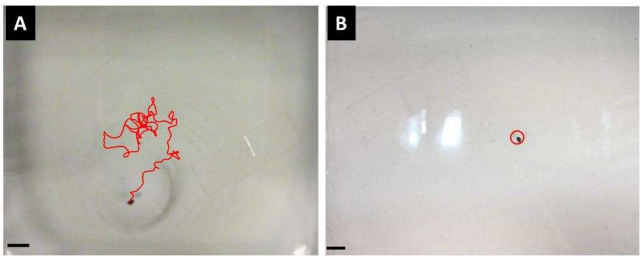

Figure 2. Trajectories of MoS_2 based motors in water. A) Translational motion of a MoS_2 based motor for 10s. B) Rotational motion of a MoS_2 based motor for 2 s. Scale bars are 1 cm.

The anisotropic distribution of sodium intercalated in MoS_2 will lead to a concentration gradient of reaction products around the particle during the exfoliation process in water. However, at such large length scale, the effect of diffusiophoresis is no longer significant as that at low Reynolds number regime.[43] Control experiment using lithium intercalated MoS_2 prepared with t-butyl

lithium as lithiation agent demonstrated that they did not exhibit any movement in water, which further rules out propulsion by concentration gradient (SI video-3). Since the MoS_2 particles only move at the air/water interface, we propose that the motion is mainly due to Marangoni effect. The naphthalene used in the preparation procedure is an organic compound existing as white crystalline solid, which has a solubility of 31.6 mg/L in water at 25°C. The motion of a droplet or solid grain at an interface driven by Marangoni effect has been extensively reported. [44-4649] Surface tension gradients brought about by the anisotropic distribution of the surface tension altering material around the droplet or grain exterior provide the driving force for the self-motion. Control experiments using acetylnaphthalene (SI video-4) and dihydroxynaphthalene (SI video-5) demonstrated the ability of naphthalene derivatives, which are solid grains, to exhibit self-propulsion on the surface of water. The motion is due to the non-uniform distribution of the organic molecules that develops asymmetrically from the solid. The resulting surface tension heterogeneity will induce motion along the chemical gradient. Similarly, for the MoS_2 based motor, the naphthalene molecules that develops from the anisotropically distributed naphthalene in MoS_2 generates a surface tension gradient around the particle and thus results in a propulsive force for the motion. A region of higher surface tension means greater intermolecular forces. The liquid with a higher surface tension pulls more strongly on the surrounding liquid than one with lower surface tension. As a result, the surface tension gradient will cause the object to be propelled towards regions of higher surface tension, where there is a region of lower density distribution of naphthalene. Figure 3 illustrates the simultaneous motion and exfoliation of the MoS_2 particle. The motion and exfoliation are in fact two separate processes due to two different components contained in the MoS_2 particle. Exfoliation is attributed to the reaction between intercalated sodium and water while motion is due to the asymmetric distribution of naphthalene on the water surface. When immersed in water, the two processes occurred at the same time, resulting in concomitant exfoliation and motion of the MoS_2 particles. The MoS_2 based motor presented here provides a strategy for preparation of TMDC based motors by encapsulating surface tension altering reagents inside. The Marangoni effect induced motion can be performed in aqueous environment without adding surfactant and external fuel. The exfoliation during motion provides substantial 2D MoS_2 nanosheets for subsequent processing steps. Combination of the mobility of the MoS_2 based motor and their autonomous exfoliation into 2D layers offers a new platform for possible applications.

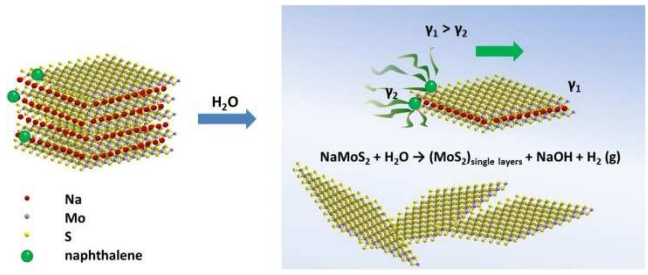

Figure 3. Schematic diagram illustrating the simultaneous self-exfoliation and autonomous motion of the MoS_2 based motor in water.

The different motion modes of the MoS_2 particles are ascribed to the differences in the shape of the particles and distribution of naphthalene in them. The solubility of naphthalene is very low and only a small amount of naphthalene at the water interface can induce the surface tension gradient required for the motion of the particle. On the other hand, the exfoliation of the particle only takes a very short time. As such, unlike the motion of agglomerates only constituted of diphenylhydrazine,[45] the amount of organic surface altering material naphthalene is not the deciding factor of the lifetime of the MoS_2 based motor. The lifespan is directly determined by the time taken for exfoliation of the whole particle, whereas the mobility of the particle is mainly related to the distribution of naphthalene. The velocity of the particle depends on the concentration gradient of naphthalene developing from that in the MoS_2 particle. Figure 4 shows the distribution of instantaneous speeds of the particle in Figure 2A against time. The speed is calculated by the means of dividing the distance covered by the amount of time taken between sequential video frames (30 frames/s). Although fluctuation occurs, gradual release of naphthalene leads the majority of the instantaneous speed of the tracked MoS_2 based motor to distribute in the region of around 3 cm/s. However, as the concentration of naphthalene increases on the surface of water during the motion, the velocity shows a slightly decreasing trend with time due to a reduction of surface tension gradient around the particle. When reaching a temporal equilibrium state, the particle can stall for a moment. Once the balanced state is broken by the changes in the distribution of the naphthalene layer, the particle will resume motion. The average speed obtained from 20 MoS_2 based motors during the first 10s is about 2.3 cm/s.

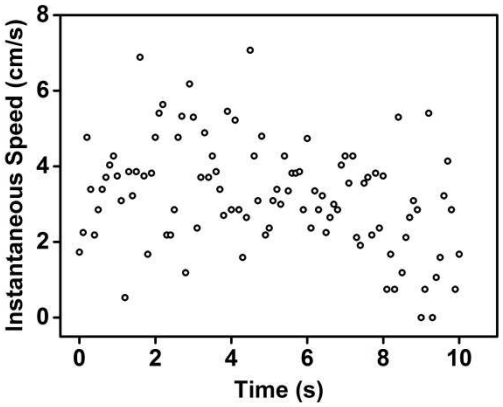

Figure 4. Instantaneous speed of the MoS_2 based motor in Figure 2A over 10s. Time interval is 0.1s.

Conclusions

In conclusion, we describe the simultaneous motion and exfoliation of a MoS_2 based motor, in which naphthalene is used to induce surface tension gradient at the water interface for propulsion and intercalated sodium reacts with water to separate the material layers. Marangoni effect provides a strategy to prepare TMDC based motors that can move autonomously in aqueous environment without additional surfactants and fuel. The unique properties of MoS_2 offer a lot of potential biomedical applications after rational functionalization. The MoS_2 motor is envisioned to be involved in performing tasks such as sensing and cargo delivery. The simultaneously exfoliated materials can be used for subsequent downstream analysis and cargo release process. The MoS_2 motor also has the potential to be used as recyclable on-the-fly extractants for removal of heavy metals in aqueous media.

M. P. acknowledge Nanyang Technological University and Singapore Ministry of Education Academic Research Fund AcRF Tier 1 (2013-T1-002-064, RG99/13) for the funding support. Z.S. was supported by specific university research (MSMT No. 20/2015).

Notes and references

[a] Division of Chemistry & Biological Chemistry, School of Physical and Mathematical Sciences, Nanyang Technological University, Singapore 637371, Singapore. pumera.research@gmail.com

[b] Department of Inorganic Chemistry, University of Chemistry and Technology Prague, Technická 5, 166 28 Prague 6, Czech Republic.

† Electronic Supplementary Information (ESI) available: [Detailed experimental procedures, AFM images and SI videos 1-5]. See DOI: 10.1039/c000000x/

1 Q. W. Wang, K. Kalantar-Zadeh, A. Kis, J. N. Coleman and M. S. Strano, *Nat. Nanotechnol.*, 2012, **7**, 699.
2 J. A. Wilson and A. D. Yoffe, *Adv. Phys.*, 1969, **18**, 193.
3 A. D. Yoffe, *Adv. Phys.*, 1993, **42**, 173.
4 M. Pumera, Z. Sofer and A. Ambrosi, *J. Mater. Chem. A*, 2014, **2**, 8981.
5 E. Benavente, M. A. Santa Ana, F. Mendizábal and G. González, *Coord. Chem. Rev.*, 2002, **224**, 87.
6 R. A. Neville and B. L. Evans, *Phys. Status Solidi B*, 1976, **73**, 597.
7 T. S. Li and G. L. Galli, *J. Phys. Chem. C*, 2007, **111**, 16192.
8 G. Eda, H. Yamaguchi, D. Voiry, T. Fujita, M. Chen and M. Chhowalla, *Nano Lett.*, 2011, **11**, 5111.
9 Y. Yoon, K. Ganapathi and S. Salahuddin, *Nano Lett.*, 2011, **11**, 3768.
10 R. Fivaz and E. Mooser, *Phy. Rev.*, 1967, **163**, 743.
11 S. Bertolazzi, J. Brivio and A. Kis, *ACS Nano*, 2011, **5**, 9703.
12 B. Radisavljevic, A. Radenovic, J. Brivio, V. Giacometti and A. Kis, *Nat. Nanotechnol.*, 2011, **6**, 147.
13 S. Das, H. –Y. Chen, A. V. Penumatcha and J. Appenzeller, *Nano Lett.*, 2013, **13**, 100.
14 H. Zeng, J. Dai, W. Yao, D. Xiao and X. Cui, *Nat. Nanotechnol.*, 2012, **7**, 490.
15 K. F. Mak, K. He, J. Shan and T. F. Heinz, *Nat. Nanotechnol*., 2012, **7**, 494.
16 H. S. Lee, S. -W. Min, Y. -G. Chang, M. K. Park, T. Nam, H. Kim, J. -H. Kim, S. Ryu and S. Im, *Nano Lett*., 2012, **12**, 3695.
17 K. S. Novoselov, D. Jiang, F. Schedin, T. J. Booth, V. V. Khotkevich, S. V. Morozov and A. K. Geim, *Proc. Natl Acad. Sci. USA*, 2005, **102**, 10451.
18 C. Lee, H. Yan, L. E. Brus, T. F. Heinz, J. Hone and S. Ryu, *ACS Nano*, 2010, **4**, 2695.
19 K. F. Mak, C. Lee, J. Hone, J. Shan and T. F. Heinz, *Phys. Rev. Lett.*, 2010, **105**, 136805.
20 P. Joensen, R. F. Frindt and S. R. Morrison, *Mater. Res. Bull.*, 1986, **21**, 457.
21 J. N. Coleman, M. Lotya, A. O'Neill, S. D. Bergin, P. J. King, U. Khan, K. Young, A. Gaucher, S. De, R. J. Smith, I. V. Shvets, S. K. Arora, G. Stanton, H. Y. Kim, K. Lee, G. T. Kim, G. S. Duesberg, T. Hallam, J. J. Boland, J. J. Wang, J. F. Donegan, J. C. Grunlan, G. Moriarty, A. Shmeliov, R. J. Nicholls, J. M. Perkins, E. M. Grieveson, K. Theuwissen, D. W. McComb, P. D. Nellist and V. Nicolosi, *Science*, 2011, **331**, 568.
22 Z. Zeng, Z. Yin, X. Huang, H. Li, Q. He, G. Lu, F. Boey and H. Zhang, *Angew. Chem. Int. Ed*., 2011, **50**, 11093.
23 A. Ambrosi, Z. Sofer, M. Pumera, *Small*, 2015, **11**, 605.
24 A. Zak, Y. Feldman, V. Lyakhovitskaya, G. Leitus, R. Popovitz-Biro, E. Wachtel, H. Cohen, S. Reich and R. Tenne, *J. Am. Chem. Soc.*, 2002, **124**, 4747.
25 R. B. Somoano, V. Hadek and A. Rembaum, *J. Chem. Phys.*, 1973, **58**, 697.
26 R. A. Gordon, D. Yang, E. D. Crozier, D. T. Jiang and R. F. Frindt, *Phy. Rev. B*, 2002, **65**, 125407.
27 A. A. Jeffery, C. Nethravathi and M. Rajamathi. *J. Phys. Chem. C*, 2014, 118, 1386-1396.
28 S. S. Chou, M. De, J. Kim, S. Byun, C. Dykstra, J. Yu, J. Huang and V. P. Dravid, *J. Am. Chem. Soc.*, 2013, **135**, 4584.
29 T. Liu, C. Wang, W. Cui, H. Gong, C. Liang, X. Shi. Z. Li, B. Sun and Z. Liu, *Nanoscale*, 2014, **6**, 11219.
30 T. Liu, C. Wang, X. Gu, H. Gong, L. Cheng, X. Shi, L. Feng, B. Sun and Z. Liu, *Adv. Mater.*, 2014, **26**, 3433.
31 C. Zhu, Z. Zeng, H. Li, F. Li, C. Fan and H. Zhang, *J. Am. Chem. Soc.*, 2013, **135**, 5998.
32 T. Wang, R. Zhu, J. Zhuo, Z. Zhu, Y. Shao and M. Li, *Anal. Chem*., 2014, **86**, 12064.
33 M. Pumera, A. H. Loo, *Trends. Anal. Chem*. 2014, **61**, 49.
34 A. E. Gash, A. L. Spain, L. M. Dysleski, C. J. Flaschenriem, A. Kalaveshi, P. K. Dorhout, S. H. Strauss. *Environ. Sci. Technol.*, 1988, **32**, 1007.
35 J. G. S. Moo, M. Pumera, *Chem. Eur. J.* 2015, **21**, 58.
36 S. Sanchez, L. Soler and Katuri, J. *Angew. Chem. Int. Ed*., 2015, **54**, 1414.
37 R. Liu and A. Sen, *J. Am. Chem. Soc.*, 2011, **133**, 20064.
38 W. Gao, A. Pei, R. Dong and J. Wang, *J. Am. Chem. Soc.*, 2014, **136**, 2276.
39 W. Gao, M. D'Agostino, V. Garcia-Gradilla, J. Orozco and J. Wang, *Small*, 2013, **9**, 467.
40 J. Zheng, H. Zhang, S. Dong, Y. Liu, C. T. Nai, H. S. Shin, H. Y. Jeong, B. Liu and K. P. Loh, *Nat. Commun*., 2014, **5**, 2995.
41 H. Li, G. Lu, Z. Yin, Q. He, H. Li, Q. Zhang and H. Zhang, *Small*, 2012, **8**, 682.
42 J. Heising and M. G. Kanatzidis, *J. Am. Chem. Soc*., 1999, **121**, 11720.
43 H. Zhang, W. Duan, L. Liu and A. Sen, *J. Am. Chem. Soc.*, 2013, **135**, 15734.
44 S. Nakata, Y. Doi and H. Kitahata, *J. Colloid Interface Sci*., 2004, **279**. 503.
45 G. Zhao, E. J. E. Stuart and M. Pumera, *Phys. Chem. Chem. Phys*., 2011, **13**, 12755.
46 G. Zhao, T. H. Seah and M. Pumera, *Chem. Asian J.* 2012, **7**, 1994.
47 G. Zhao, T. H. Seah and M. Pumera, *Chem. Eur. J.*, 2011, **17**, 12020.
48 Y. Sumino, H. Kitahata, K. Yoshikawa, M. Nagayama, M. N. Schin-ichiro, N. Magome and Y. Mori, *Phys. Rev. E*, 2005, **72**, 041603.
49 J. Orozco, D. Vilela, G. Valdés-Ramírez, Y. Fedorak, A. Escarpa, R. Vazquez-Duhalt and J. Wang, *Chem. Eur. J.*, 2014, **20**, 2886.

